doi.org/10.1109/TAP.2013.2269473

Active UWB Reflector for RFID and Wireless Sensor Networks

A. Lazaro, *Member, IEEE,* A. Ramos, R.Villarino, D.Girbau, *Senior Member, IEEE*

***Abstract*—In this paper, we present an active ultra-wideband (UWB) reflector for Radio Frequency Identification (RFID) and wireless sensor applications. The tag is composed of a receiver UWB antenna connected to a broadband amplifier. Its output is connected to a cross-polarized transmit antenna. In order to increase the battery lifetime, an UHF link is used to wake up the microcontroller. It modulates the radar cross section of the tag by turning the amplifier bias on and off. The amplitude of the reflected UWB pulse sent by the UWB reader is modulated as a result. The basic theory of operation of ultra-wideband radio identification systems is explained in this paper. A proof of concept using commercial components and experimental results obtained with an ultra-wideband radar are presented.**

***Index Terms*—RFID, UWB, Active Antennas, Transponder**

I. INTRODUCTION

Ultra-wideband (UWB) tags for Radiofrequency Identification (RFID) systems may be a good alternative for low-cost item tagging, as recently demonstrated in [1-4]. Printable chipless RFID tags based on multiresonators have been reported in [1][2], where the information is coded in frequency domain. An alternative method where the information is coded in time delay has been proposed in [3-8]. However, in chipless RFID the range and the number of bits suitable to be coded are limited [5-8]. Several RFID-based localization systems have also been proposed for different applications in recent years, such as emergency rescuing, patient tracking, asset and livestock tracking, and many other areas [9-13]. There are different approaches for local positioning. A comparison between some of these is made in [12]. UWB systems can so far deliver an accuracy of few cm [14-16].

In many applications (e.g., inventory items, smart sensors or surveillance systems) it is desirable to have very low complexity (low cost), long range, and low power consumption tags. This study presents an active UWB reflector in order to reduce the complexity of the tag. The goal is to increase the radar cross section (RCS) of the tag by providing it with gain. This idea has been used in the active reflectors proposed as an active radar calibrator in the literature [17]. Passive and active Van Atta Arrays have been proposed for narrow band RFID applications [18-19]. In this paper, the reflector consists of one receiver UWB antenna followed by a UWB amplifier connected through a delay-line to a transmitter UWB antenna. The reader is based on a UWB Impulse Radar (IR). In order to increase the battery life time, the tag remains in a low power state when it is not interrogated by the reader. The working principle is as follows: the reader activates the tag by sending a modulated tone on the UHF band (868 MHz) that is detected with a diode detector. Once the tag is awakened, the reader sends a UWB pulse. The tag receives the pulse, amplifies it and retransmits it. The amplifier enables the range to be increased and detected compared to a complete backscattering passive reflector [3,6-7]. This tag is simpler than other active tags or reflectors [14,20-23], because it does not require complex synchronization techniques between the pulse generator –included in the tag and the receiver in the reader [23]. Several low-noise integrated amplifiers for UWB have been reported in the literature (a comparison is given in [24], Table III) and they can be used for these purposes. These amplifiers achieve power consumptions between 1.3 mW to 25 mW, depending on the CMOS process, topology and gain. The tag therefore needs no special integrated designs. A proof of concept using commercial components is presented here.

The paper is organized as follows. Section II describes the system architecture, the basic theory of operation and the implementation of an active tag based on active UWB reflector. This section also presents a link budget of the system. Section III presents the experimental results and finally, Section IV draws the conclusions.

Manuscript received October 23, 2012. This work was supported by the Spanish Government Project TEC2011-28357-C02-01. A. Lazaro, A. Ramos, R:.illarino and D. Girbau members of the Electronics, Electrical and Automatics Engineering Department, Universitat Rovira i Virgili, 43007 Tarragona, Spain (antonioramon.lazaro@urv.cat, phone: +34-977.55.86.68).

II. SYSTEM DESIGN

A. System architecture

The proposed system is shown in Fig. 1. It comprises a reader and the tags. First, the reader interrogates the tag using a UHF (868 MHz) signal, which wakes up the tag logic circuitry. This signal is modulated using an On-Off Keying (OOK) Pulse-Width Modulation (PWM) schema in order to prevent false wake ups due to the presence of other UHF communication systems near the tag. This scheme also allows the reader to send commands to the tag or implement more sophisticated anti-collision protocols. The UHF modulator is implemented with an UHF oscillator. A variable attenuator (NVA2500V35 from Minicircuits) is used to control the transmitted power and to modulate the signal. Finally, the signal is amplified using a buffer amplifier (Gali84+ from

Minicircuits), followed by a power amplifier (RF3809 from RF Monolithic Solutions).

In order to read the tag response, the reader then sends a UWB pulse to the tag and samples the reflected pulse. A PulsON P400 MRM commercial UWB radar from Time Domain is used for the UWB link. This radar complies with FCC regulations and sends a UWB pulse centered at 4.3 GHz with a bandwidth of 1.35 GHz. The transmit pulse repetition rate (PRF) is 10.1 MHz. The reader uses two cross-polarized Vivaldi antennas.

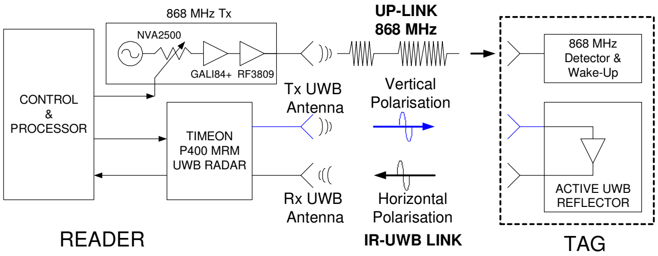

Fig. 1. UWB/UHF hybrid RFID system with UHF up-link and IR-UWB link.

Fig. 2 shows the block diagram of the tag and Fig. 3 shows a photograph of the tag and the experimental setup. The tag size is 133 mm×133 mm. The wake-up detector consists of an envelope detector based on the Avago HSM2852 Schottky diodes and a matching network tuned at 865-868 MHz. A low-power microcontroller (PIC16F1827 from Microchip) is used to implement the tag logic part. This demodulates the signal from the output of the envelope detector (using one of its internal comparators) and controls a MAX4715 switch from Maxim, which is connected to the amplifier supply. Once the tag is awakened by the reader, the reader sends a UWB pulse towards the tag, which is amplified and retransmitted by the tag using the other polarization. The microcontroller modulates the amplitude of the UWB pulse by controlling the bias voltage of the UWB amplifier. A commercial MMIC from Avago (ABA31563) is used here. The amplifier consumes 13 mA at 3 V (39 mW). Fig. 4 shows the communication protocol used. First, the reader wakes up the tag using the UHF link. Then, the reader sends a UWB pulse and receives the backscattered answer. Next, it sends a new command to the tag via the UHF link to request the following bit, and so on. Note that the time-of-flight (TOF) is measured by the radar. No special synchronization between the tag and the reader is therefore required. This point is an important difference compared to other IR-UWB tags that use a pulse transmitter implemented in the tag instead of an amplifier [20-21]. The pulse transmitter should be synchronized with the reader in these systems. In addition, this tag is compatible with any UWB receiver (carrier based or IR based) because it acts as an active reflector. The increase in power consumption may be prohibitive for completely passive tags. However, it is acceptable for semipassive tags, since the sensors also need DC current to operate and the amplifier is turned off after the data transmission. The DC power consumption of the tag is comparable or lower than other wireless systems such as Zigbee, but this system can also be combined with localization techniques based on TOF. After answering the reader, the tag remains in sleep mode, in which consumption is less than 100 nA (not including the sensors' consumption).

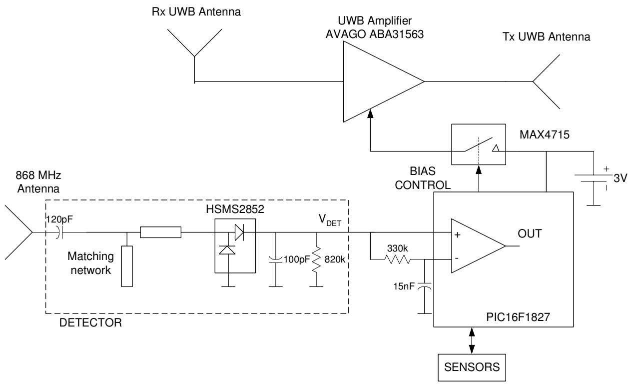

Fig. 2. Block diagram of the tag based on an active reflector.

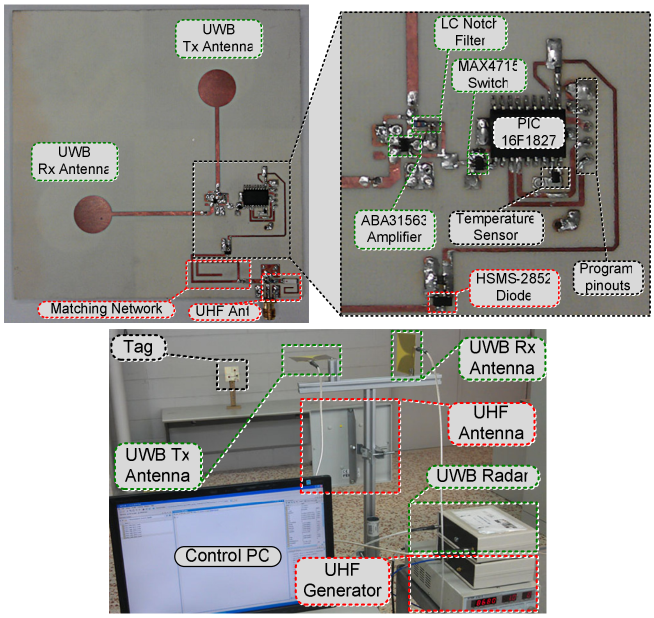

Fig. 3. Photograph of the implemented tag (top) and experimental setup (bottom).

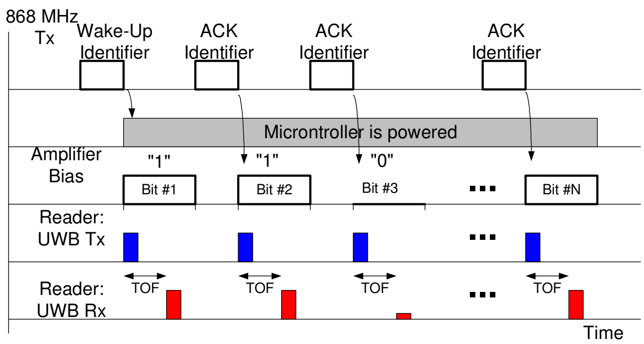

Fig. 4. Communication protocol.

B. *Tag Antennas*

Two orthogonal circular slot UWB antennas similar to the one from [7] were used in the tag. The outer and the inner diameters are 36 mm and 18 mm respectively. The ground plane dimensions are 70 mm width per 50 mm height. The simulated reflect coefficient (S_{11}), gain and coupling (S_{21}) are shown in Fig. 5. The separation between the antennas is established at 40 mm from the feed points, in order to reduce coupling between them below -20 dB in the amplifier band. The simulations were performed with Agilent Momentum. Although the coupling between the cross-polarized antennas is low in the tag and the reader, and the clutter level reduction is important, the utilization of cross-polarized antennas has the drawback that the tag must be well-oriented to the reader to prevent losses due to depolarization. In applications where the tag orientation is unknown, circular polarized antennas could be used in the tag or the reader end. Standard circularly-polarized patch antennas such as the ones used in commercial UHF RFID applications [25] can be used at the UHF link. Circular polarized UWB antennas such as sinuous or spiral antennas can be used at the UWB link. In addition, the UWB antennas in the tag could be replaced by printed circular polarized antennas [26].

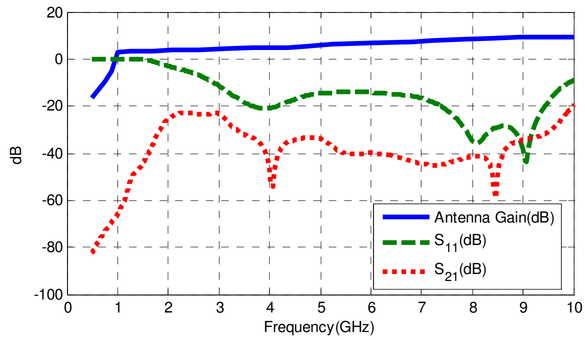

Fig. 5. Simulated antenna gain, reflection coefficient and coupling between Tx and Rx tag antennas.

In order to save space, a ceramic antenna (model P/N 0868AT43A0020 from Johanson Technology) was connected to the input of the UHF detector. The antenna has a peak gain of -1dB in the 868 MHz band. A matching network composed of a 15 nH series inductor and 4.7 pF capacitor in parallel connected to ground was used to tune the antenna in the 865-868 MHz band.

C. *UWB Amplifier*

As mentioned above, the commercial MMIC from Avago ABA31563 is used in this prototype. Fig. 6 shows the measured S parameters for the bias point of 3 V, 13 mA of current. The tag was able to oscillate due to limited coupling between the tag's antennas. Fig. 7 shows the open loop gain computed from the cascade simulation of the amplifier and the antennas coupling. It can be seen that the open loop gain could increase by 20 dB around 2 GHz due to the high gain of the amplifier. The separation between antennas should be increased to minimize coupling and therefore to avoid oscillation, but the tag size would also increase. Another solution is to insert a notch filter to reduce the gain. A simple LC series notch filter implemented with a transmission line (4 mm long and 0.5 mm wide) loaded with a 3 pF capacitor is used in this work. The notch filter can be easily tuned to 2 GHz in order to reduce the gain, as shown in Fig. 7.

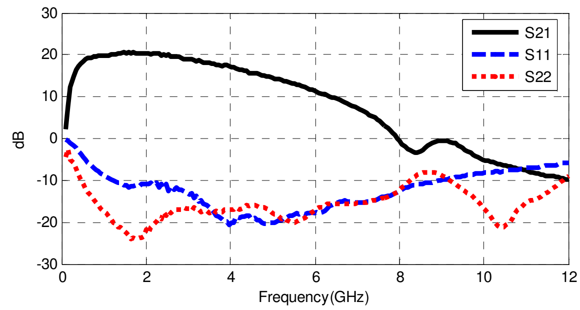

Fig. 6. Measured S parameters of the amplifier.

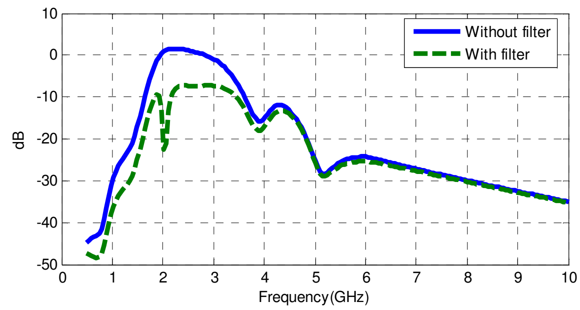

Fig. 7. Open loop gain without filter (solid line) and with notch filter (dashed line).

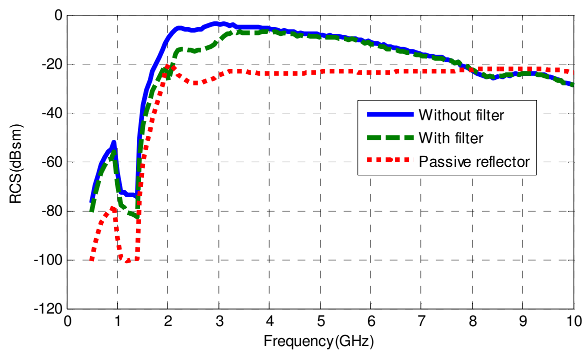

Fig. 8. Simulated RCS as function of the frequency without (solid line) and with the notch filter (dashed line).

The amplitude of the modulated reflected pulse is a function of the RCS of the reflector. The RCS of the active reflector can be computed using [17]:

$$\sigma = \frac{\lambda^2}{4\pi} G_{tag,r} G_a G_{tag,t} \tag{1}$$

where λ is the wavelength, $G_{tag,r}$, $G_{tag,t}$ are the tag receiver and transmitted antenna gains, respectively, and G_a is the amplifier gain including the notch filter.

Fig. 8 shows the RCS computed using (1) without and with the filter. As expected, a reduction of the RCS around the center frequency of the notch filter is achieved, which decreases when the frequency moves away from the filter central frequency. For instance, a loss due to the filter of 1.4 dB at 4 GHz (which is around the 4.3 GHz central frequency of the reader's UWB pulse) is shown. At 4 GHz, a RCS peak of -7 dBsm is obtained and the RCS is almost flat around the central frequency of the pulse spectrum. The increase in the RCS compared to a passive reflector or tag is clearly visible.

D. *Down link budget*

The bit error rate of the UWB link depends on the ratio between the energy per bit to noise spectral density (E_b/N_0). UWB radar can improve the E_b/N_0 by using coherent integration of pulses. If N_s pulses are integrated every T_b seconds, the bit rate can be written as $r = PRF/N_s$, where PRF is the pulse repetition frequency. The signal to noise ratio (S/N) can be expressed as [27]:

$$\frac{S}{N} = \frac{\frac{E_b}{T_b}}{N_0 B} = \left(\frac{E_b}{N_0}\right)\frac{PRF}{N_s B} \tag{2}$$

where B is the channel bandwidth of the system (defined by the bandwidth of the UWB pulse and by the frequency response of all of the antennas).
Then, the E_b/N_0 in dB can be expressed as:

$$\left(\frac{E_b}{N_0}\right)_{dB} = \left(\frac{S}{N}\right)_{dB} + PG(dB) \tag{3}$$

where the processing gain is defined as:

$$PG(dB) = 10\log\left(\frac{B}{PRF}\right) + 10\log(N_s) \tag{4}$$

The processing gain (PG) depends on the bit rate and the pulse repetition rate, which are parameters that depend on the target application.
The noise spectral density N_0 is a function of the noise factor:

$$N_0 = kT_0F \tag{5}$$

and the average receiver power can be obtained from the radar equation:

$$S = \frac{P_t}{4\pi r^2} G_t \sigma \frac{1}{4\pi r^2} \frac{\lambda^2}{4\pi} G_r \tag{6}$$

where the RCS of the active reflector is given by (1) and r is the tag-to-reader distance.

Fig. 9 shows the E_b/N_0 calculated with the equations above. For the simulations, an amplifier with a gain of 16 dB, and two UWB reader antennas with a gain of 6 dB were considered. The tag antennas are simulated with Agilent Momentum. The simulated average gain of 5 dBi in the band of interest, and a half power beam width (HPBW) of approximately 64º and 50º in the E-plane and H-plane, respectively. The calculation was performed at the central frequency (4.3 GHz) of the pulse and a 1.35 GHz bandwidth was taken into account. The average equivalent radiated power used is -14.5 dBm (FCC 15b compliant) and the PRF is 10.1 MHz. Assuming a bit error limit of 10^{-3}, an E_b/N_0 of 6.8 dB is required for Binary Phase Shift Keying (BPSK) demodulation. From this simulation, depending on the number of samples N_s (1, 64, 4096 or 32768 can be used with the P400 radar), read ranges of 3.6 m, 9.5 m, 27.5 m and 45.5 m can be theoretically achieved, respectively. The maximum read range for a bit error rate BER=10^{-3} as a function of the illumination angle in the E and H planes are shown in Fig.10 for the case N_s=32768. A solution to reduce the dependence on the illumination angle is to use omnidirectional UWB antennas at the tag. Fig.11 shows the E_b/N_0 calculated assuming the UWB antenna gain equal to 0 dBi. A comparison with the case of a passive tag (G_a=1) [28-29] is also included. In this case, the active approach indicates a read range of about 25 m compared with 12 m of the passive approach.

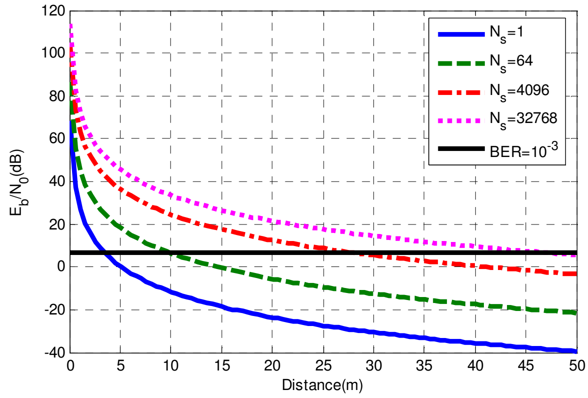

Fig. 9. Simulated E_b/N_0 as a function of the distance for different integration sampling numbers (N_s=1, 64, 4096, and 32768). The limit line for BER=10^{-3} (E_b/N_0=6.8 dB) is also indicated.

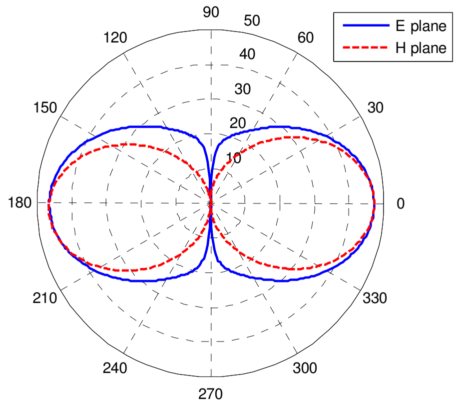

Fig.10. Simulated maximum read range (in meters) corresponding to BER=10^{-3} as a function of the illumination angle in the E plane (solid line) and H plane (dashed line). The reader UWB antenna gain is assumed 6 dBi and the integration sampling number N_s=32768.

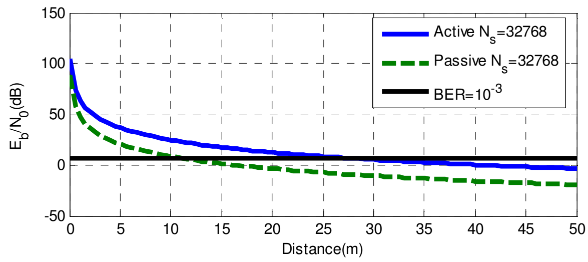

Fig.11. Simulated E_b/N_0 as a function of the distance for an active reflector (solid line) and a passive reflector (dashed line). The reader UWB antenna gain is assumed 0 dBi and the integration sampling number N_s=32768. The limit line for BER=10^{-3} (E_b/N_0=6.8 dB) is also indicated.

E. Uplink Link budget

Fig. 12 shows the measured voltage detected by the diode detector as a function of the input power. The tangential sensitivity (TSS) is the lowest input signal power level for which the detector will have an 8 dB signal-to-noise ratio at the output of a test video amplifier. A TSS value of to -57 dBm is typically obtained using these zero bias diodes [30]. Setting the sensitivity of the wake-up system to -40 dBm (3 mV of detected voltage) would therefore be enough to ensure a good link quality. Fig. 13 shows the power received at the detector as a function of the distance. To avoid the uplink limiting the read range, the maximum wake-up distance should be larger than 45.5 m in free space (simulated limit for the UWB link). A detector on the 2.45 GHz ISM band cannot achieve this distance considering the maximum permitted power by regulations. The UHF band was chosen for this reason. Using the maximum power transmitted under European (ETSI EN 302 208) and USA (FCC-15) RFID regulations, a distance larger than 70 m can be obtained in free space. A wake-up antenna gain of -1dB was considered in the calculations. Since the wake-up distances are much larger than the maximum read range limited by the UWB link, there is consequently a fading margin to mitigate multipath effects in the UHF channel. The data rate is limited by the low-pass filter at the output of the detector and by the speed of internal comparator in the microcontroller. In the experiments the data rate used is 1 kHz, however can be increased up to 40 kHz. These speeds are high enough to send small configuration commands for sensor applications.

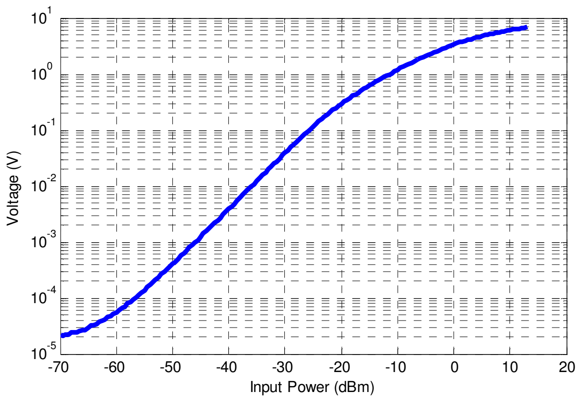

Fig.12. Measured detected voltage as a function of the input power at 868 MHz.

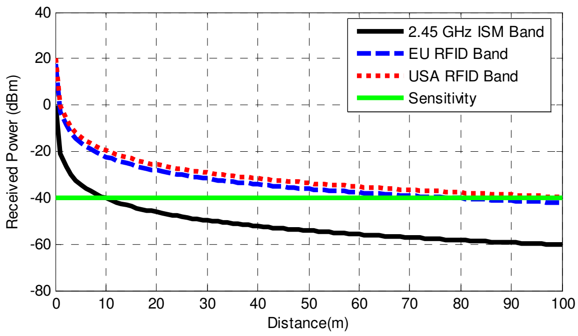

Fig. 13. Received power as a function of the tag to reader distance for the uplink.

III. EXPERIMENTAL RESULTS

We conducted experiments in the laboratory in order to check the system at tag-to-reader distances of 1 m and 10 m. Figs. 14-15 show the UWB signal received after background subtraction was applied as a function of the delay for a tag located 1 m and 10 m away from the reader, respectively. A small reflection due to the tag structure is observed when the amplifier is biased Off (State Off). In contrast, there is a strong reflection when the amplifier is biased On (State On). A small delay is observed between the two states due to the propagation delay through the amplifier. Multiple reflections are also observed for the State On due to feedback coupling between the tag antennas. Of course, at a distance of 10 m the level of received signal is smaller than for 1 m, and consequently the signal-to-noise ratio decreases.

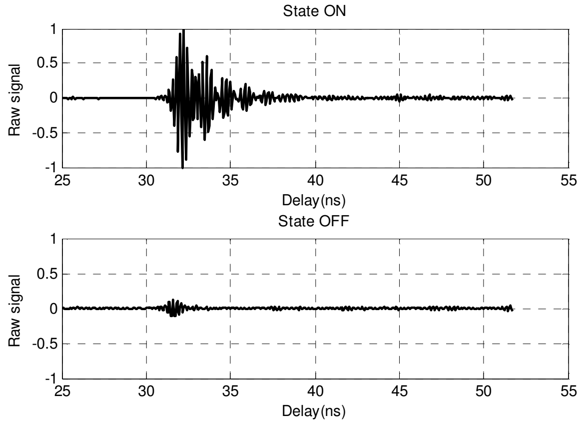

Fig. 14. Normalized received UWB raw signal as a function of time delay for the two states (amplifier On and Off) at a tag-to-reader distance of 1m.

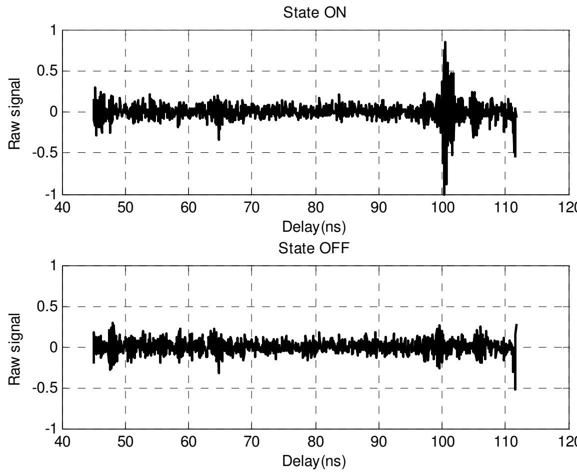

Fig. 15. Normalized received UWB raw signal as a function of time delay for the two states (amplifier On and Off) at a tag-to-reader distance of 10 m.

A matched filter technique can be applied in order to maximize the signal-to-noise ratio. This well known detection technique is based on detecting of the peak at the output of a correlation between the signal with an optimum signal template. This optimum template depends on the antennas used in the reader and the tag, and the transmitted pulse.

Although it can be characterized, this template would change between tag or reader models in real applications. To solve this drawback, a technique based on the Continuous Wavelet Transform (CWT) can be applied [7]. This technique exploits the denoising properties of the CWT and it can be seen as an implementation of a matched filter without any need to know any template signal a priori. As explained in detail in [7], a complex Gaussian Wavelet of 3rd order is chosen. Figs. 16-17 show the normalized magnitude of the CWT applied to the received signal for 1 m and 10 m, respectively. In both cases, the received signal for State On is clearly detectable for both distances. For the State Off, the tag is not retransmitting the reader's pulse. The signal received therefore consists of background and residual clutter.

A differential schema encoding can be adopted in order to remove the clutter. For each signal, we subtract the first signal of an 8-bit sequence. If the first state of any sequence is always the same, the full sequence can be obtained.

Figs. 18-20 show the maximum magnitude of the CWT applied to the received signal after subtracting the received signal for the first bit. An arbitrary bit sequence (0101011) is transmitted which could correspond to a sensor data connected to the microcontroller, or an identifier code.). In order to verify the simulations of Fig. 9, measurement in outdoor environment has been performed at a 45 m distance. The result for the same sequence is shown in Fig. 20. Although the effect of noise and clutter is clearly visible, the bit sequence can be demodulated. These figures show that the bit sequence can be demodulated using a simple threshold comparator at 50% of the maximum amplitude of all the signals of the sequence. The time delay of the peak for the "On" States depends on the time-of-flight delay between the tag and the reader, added to a small systematic delay between the reader and its own antennas. This small delay due to the reader's antennas is known and always the same for any tag-to-reader distance. This active reflector could thus be combined with localization techniques by using multiple readers located at different known positions (anchors).

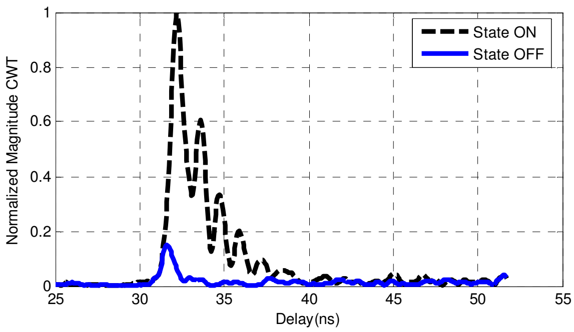

Fig. 16. Normalized maximum of CWT as a function of time delay for the two states (amplifier On and Off) at a tag-to-reader distance of 1 m.

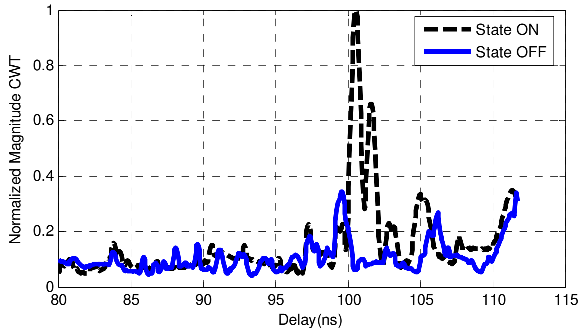

Fig. 17. Normalized maximum of CWT as a function of time delay for the two states (amplifier On and Off) at a tag-to-reader distance of 10 m.

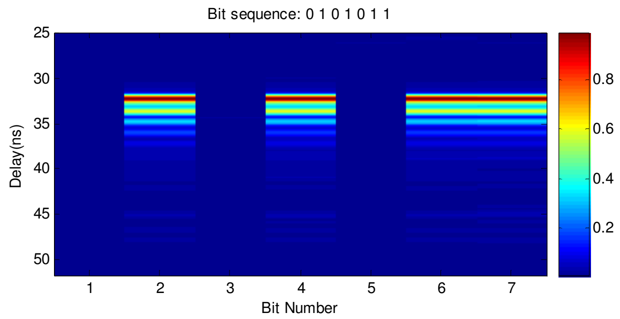

Fig. 18. Normalized maximum of CWT as a function of time delay for a bit sequence at a tag-to-reader distance of 1 m (indoor envioremen).

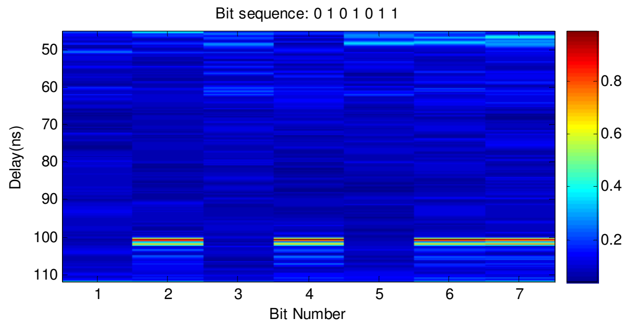

Fig. 19. Normalized maximum of CWT as a function of time delay for a bit sequence at a tag-to-reader distance of 10 m (indoor environment).

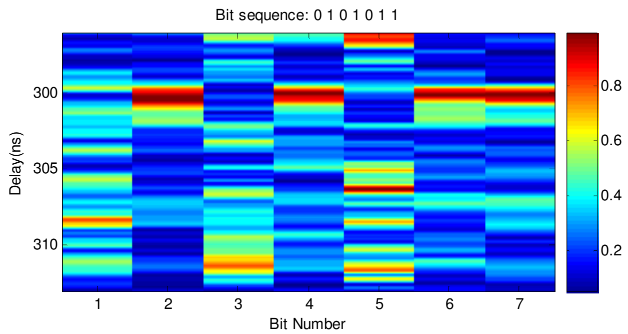

Fig. 20. Normalized maximum of CWT as a function of time delay for a bit sequence at a tag-to-reader distance of 45 m (outdoor environment).

IV. CONCLUSION

In this paper, we present the basic operation theory of time-coded UWB RFID systems based on active reflectors. A proof of concept using a novel hybrid UWB-UHF RFID system is described. The UHF link is used to waken the tag, whereas the active reflector is used to modulate the UWB pulse sent by the reader. The reader's pulse is amplified and retransmitted back with cross-polarization from the tag to the reader. A UHF link is chosen instead of an ISM link (2.45 GHz) to achieve longer wake-up distances. The read range of the system is theoretically limited by the UWB link to 45.5 m in free space. The use of cross-polarized antennas helps to reduce both clutter interference and coupling between antennas at the reader and the tag. In the case of the reader, it helps to exploit the dynamic range of the receiver. In the case of the tag, the coupling in-band is reduced by using different polarizations in reception and transmission. A commercial MMIC amplifier has been used in the prototype presented. Although a good performance is achieved, power consumption could be improved using UWB CMOS amplifiers. Special care must be taken in the tag design to avoid oscillations. These oscillations can appear out of the UWB band (low frequency) where the amplifier has a large gain due to the coupling between the antennas. A simple approach has been proposed, consisting of the introduction of a notch filter to reduce the open loop gain in this frequency band.

An experimental setup based on a UWB radar is used as the reader. The difficulty in detecting the scattered signal and the time-of-flight in presence of noise is demonstrated. The Continuous Wavelet transform is used as a detection technique, working as a matched filter. The benefit of this technique is that a template signal is not required in advance.

Indoor and outdoor experimental results of up to 10 m and 45 m, respectively, have been achieved to show the viability of the system. The system presented opens the door to the integration of advanced sensors and localization applications based on UWB active reflectors used as tags.

REFERENCES

[1] S. Preradovic, I. Balbin, N. Chandra Karmakar, and G. F. Swiegers, "Multiresonator-Based Chipless RFID Systemfor Low-Cost Item Tracking," *IEEE Trans. On Microwave Theory and Tech.*, Vol. 57, No. 5, pp. 1411-1419, May 2009.

[2] D.Girbau, J. Lorenzo, C.Ferrater, A. Lázaro, R. Villarino, "Frequency-Coded Chipless RFID Tag Based on Dual-Band Resonators;" *IEEE Antennas and Wireless Propagation Letters,* Vol.11, No. 1, pp.126-128, 2012.

[3] D. Dardari and R. D'Errico, "Passive Ultrawide Bandwidth RFID," *IEEE Global Telecommunications Conference (GLOBECOM)*, pp. 1-6, 2008.

[4] S. Hu, Y. Zhou, C. L. Law, and W. Dou, "Study of a Uniplanar Monopole Antenna for Passive Chipless UWB-RFID Localization System," *IEEE Trans. On Antennas and Prop.*, Vol. 58, No. 2, pp. 271-278, Feb. 2010.

[5] S. Preradovic, N. Karmakar, and M. Zenere, "UWB Chipless Tag RFID Reader Design," *IEEE International Conference on RFID-Technology and Applications*, 17-19 June 2010, Guangzhou, China.

[6] A. Ramos, A. Lázaro, D. Girbau, and R. Villarino, "Time-domain measurement of time-coded UWB chipless RFID tags", *Progress in Electromagnetics Research*, Vol. 116, pp. 313-331, 2011.

[7] A. Lazaro, A. Ramos, D. Girbau, and R. Villarino, "Chipless UWB RFID Tag Detection using Continuous Wavelet Transform," *IEEE Antennas and Wireless Prop. Letters*, Vol. 10, pp. 520-523, 2011.

[8] D.Girbau, A.Ramos, A.Lazaro, S.Rima, R.Villarino, "Passive Wireless Temperature Sensor Based on Time-Coded UWB Chipless RFID Tags," accepted in *IEEE Transactions on Microwave Theory and Techniques*, DOI: 10.1109/TMTT.2012.2213838

[9] J. Woochul, J. Melngailis, and R. W. Newcomb, "Disposable CMOS passive RFID transponder for patient monitoring," *IEEE International Symposium on Circuits and Systems*, pp. 5071- 5074, 2006.

[10] T. Inaba, "Value of Sparse RFID Traceability Information in Asset Tracking during Migration Period," *IEEE International Conference on RFID* , pp. 183-190, Apr. 2008.

[11] S. Pandey and D. Singh, "Efficient and Cost Effective Tracker in Monitored Area Network Using RFID," *IEEE International Conference on Wireless and Optical Comm. Network*, pp. 1-5, Apr. 2006.

[12] C. Benavente-Peces, V. Moracho-Oliva, A. Dominguez-Garcia, and M. Lugilde-Rodriguez, "Global system for location and guidance of disabled people: Indoor and outdoor technologies integration," *5th Int. Network. Services Conf.*, pp. 370-375, Apr. 2009.

[13] D. Hepeng and S. Donglin, "Indoor location system using RFID and ultrasonic sensors," *IEEE International Symposium on Antennas, Propagation and EM Theory*, pp. 1179-1181, Nov. 2008.

[14] S. Wehrli, R. Gierlich, J. Hüttner, D. Barras, F. Ellinger, and H. Jäckel, "Integrated Active Pulsed Reflector for an Indoor Local Positioning System," *IEEE Trans. On Microwave Theory and Tech.*, Vol. 58, No. 2, pp. 267-276, Feb. 2010.

[15] A. Fujii, H. Sekiguchi, M. Asai, S. Kurashima, H. Ochiai, and R. Kohno, "Impulse radio UWB positioning system," *IEEE Radio Wireless Symp. Dig.*, pp. 55-58, Jan. 2007.

[16] B. Waldmann, R. Weigel, P. Gulden, and M. Vossiek, "Pulsed frequency modulation techniques for high-precision ultra wideband ranging and positioning," *IEEE Int. Ultra-Wideband Conf.*, Vol. 2, pp. 133-136, Sep. 2008.

[17] D. R. Brunfeldt and F. T. Ulaby, "Active Reflector for Radar Calibration," *IEEE Trans. On Geoscience and Remote Sensing*, Vol.GE-22, No.2, pp.165-169, March 1984.

[18] J. A. Vitaz, A. M. Buerkle, K. Sarabandi, "Tracking of metallic Objects Using a Retro-Reflective Array at 26 GHz," *IEEE Trans. On Antennas and Prop*, Vol. 58, No.11, pp. 3539-3544, Nov. 2010.

[19] P. Chan, V. Fusco, "Bi-Static 5.8 GHz RFID Range Enhancement using Retrodirective techniques," *Proc. of the 41st European Microwave* Conference, pp. 976-979, 2011.

[20] S. Krishnan, V. Pillai, and W. Wenjiang, "UWB-IR Active Reflector for High Precision Ranging and Positioning Applications," *2010 IEEE Intl. Conf. on Communication Systems (ICCS)*, pp.14-18, 2010.

[21] D. Dardari, "Pseudo-random active UWB reflectors for accurate ranging," *IEEE Commun. Lett.*, Vol. 8, No. 10, pp. 608-610, Oct. 2004.

[22] A. Rabbachin and I. Oppermann, "Synchronization analysis for UWB systems with a low-complexity energy collection receiver," *Proc. IEEE Ultrawideband Syst. Technol. Conf., Kyoto, Japan*, pp. 288–292, 2004.

[23] M.Baghaei-Nejad, D.S.Mendoza, Z.Zou, S.Radiom, G.Gielen, Z.Li-Rong, H.Tenhunen, "A remote-powered RFID tag with 10Mb/s UWB uplink and −18.5dBm sensitivity UHF downlink in 0.18μm CMOS," IEEE Int. Solid-State Circuits Conference - Digest of Technical Papers, 2009. ISSCC 2009.,Vol., No., pp.198-199, 8-12 Feb. 2009.

[24] Z. Zou, D. Sarmiento, P. Wang, Q. Zhou, J. Mao, F. Jonsson, H. Tenhunen, and L. R. Zheng, "A Low-Power and Flexible Energy Detection IR-UWB Receiver for RFID and Wireless Sensor Networks," *IEEE Trans. on Circuits and Systems*, Vol. 58, No. 7, pp. 1470-1482, Jul. 2011.

[25] Z.N.Chen, X.Qing, and H.L.Chung, "A Universal UHF RFID Reader Antenna", *IEEE Trans. On Microwave Theory and Tech.*, Vol. 57, No. 5, pp.1275-1282, May 2009.

[26] Y.Shen, C.L. Law, and Z.She, "A CPW-fed circularly polarized antenna for lower ultrawideband applications," *Microwave and Optical Technology Letters*, Vol. 51, No. 10, pp.2365-2369, Oct.2009.

[27] M.G. diBenedetto, T. Kaiser, A.F. Molish, I. Oppermann, C. Plitano, and D. Porcino(eds.). "UWB Communications Systems: A Comprehensive Overview". EURASIP Publishing,2005. ISBN 9775945100.

[28] A.Ramos, A.Lazaro, D.Girbau, "Semi-Passive Time-Domain UWB RFID System," *IEEE Trans. on Microwave Theory and Techniques*, Vol.64, Nº4, pp.1700-1708, April 2013.
[29] R. D'Errico, M. Bottazzi, F. Natali, E. Savioli, S. Bartoletti, A. Conti, D. Dardari, N. Decarli, F. Guidi, F. Dehmas, L. Ouvry, U. Alvarado, N. Hadaschik, C. Franke, Z. Mhanna, M. Sacko, Y. Wei, A. Sibille, "An UWB-UHF Semi-Passive RFID System for Localization and Tracking Applications", *IEEE 2012 Int. Conf. on RFID –Technologies and Applications (TA), Nice (France)*, pp.18-23, 2012.
[30] Datasheet "HSMS-285x Series Surface Mount Zero Bias Schottky Detector Diodes," Avago Technologies, AV02-1377EN, 2009.

Antonio Lázaro (M'07) was born in Lleida, Spain, in 1971. He received the M.S. and Ph.D. degrees in telecommunication engineering from the Universitat Politècnica de Catalunya (UPC), Barcelona, Spain, in 1994 and 1999, respectively. He then joined the faculty of UPC, where he currently teaches a course on microwave circuits and antennas. In July 2004 he joined the Department of Electronic Engineering, Universitat Rovira i Virgili, Tarragona, Spain. His research interests are microwave device modeling, on-wafer noise measurements, monolithic microwave integrated circuits (MMICs), low phase noise oscillators, MEMS, and microwave systems.

Angel Ramos received the BS in Telecommunication Engineering and the MS in Electronic Engineering from Universitat Rovira i Virgili (URV), Tarragona, Spain, in 2010 and 2011, respectively. He is pursuing his PhD with the Department of Electronics, Electrics and Automatics Engineering, URV.

Ramon Villarino received the Telecommunications Technical Engineering degree from the Ramon Llull University (URL), Barcelona, Spain in 1994, the Senior Telecommunications Engineering degree from the Polytechnic University of Catalonia (UPC), Barcelona, Spain in 2000 and the PhD from the UPC in 2004. During 2005-2006, he was a Research Associate at the Technological Telecommunications Center of Catalonia (CTTC), Barcelona, Spain. He worked at the Autonomous University of Catalonia (UAB) from 2006 to 2008 as a Researcher and Assistant Professor. Since January 2009 he is a Full-Time Professor at Universitat Rovira i Virgili (URV). His research activities are oriented to radiometry, microwave devices and systems, based on UWB, RFIDs and frequency selective structures using MetaMaterials (MM).

David Girbau (M'04) received the BS in Telecommunication Engineering, MS in Electronics Engineering and PhD in Telecommunication from Universitat Politècnica de Catalunya (UPC), Barcelona, Spain, in 1998, 2002 and 2006, respectively. From February 2001 to September 2007 he was a Research Assistant with the UPC. From September 2005 to September 2007 he was a Part-Time Assistant Professor with the Universitat Autònoma de Barcelona (UAB). Since October 2007 he is a Full-Time Professor at Universitat Rovira i Virgili (URV). His research interests include microwave devices and systems, with emphasis on UWB, RFIDs and RF-MEMS.